Effect of DOPA and dopamine coupling on protein loading of hydroxyapatite

Vinayaraj Ozhukil Kollath,*[a,b,1] Steven Mullens,[b] Jan Luyten,[b,2] Karl Traina[a,3] and Rudi Cloots*[a]

[a] GREEnMat, Department of Chemistry, University of Liège, B6a Sart Tilman, Liège 4000, Belgium.
Fax: 32 4366 3413; Tel: 32 4366 3436; E-mail: vozhukil@alumni.ulg.ac.be; karl.traina@ulg.ac.be; rcloots@ulg.ac.be

[b] Sustainable Materials Management, Flemish Institute for Technological Research (VITO), Boeretang 200, Mol 2400, Belgium
Fax: 32 1432 1186; Tel: 32 1433 5706; E-mail: vozhukil@alumni.ulg.ac.be; steven.mullens@vito.be; jan.luyten@mtm.kuleuven.be

* Corresponding author(s)

Abstract

Hydroxyapatite (HA) is a promising carrier material for oral delivery of biomolecules such as proteins and drugs. Ways to increase the loading of such molecules on HA will lead to better nanomedicine. This study reports the surface functionalisation of HA particles using the mussel-inspired molecules dopamine (DA) and 3,4-dihydroxy-L-phenylalanine (DOPA), in order to increase protein loading. The adsorption mechanisms are discussed based on the adsorption isotherms, zetapotential, thermal analysis and theoretical models. Results show that DA functionalization enhanced the loading while DOPA functionalization was ineffective.

Keywords: hydroxyapatite; protein; dopamine; adsorption isotherm; oral delivery

Note: This is an author postprint version of the article published as: V. Ozhukil Kollath,,, S. Mullens, J. Luyten,, K. Traina, and R. Cloots. "Effect of DOPA and dopamine coupling on protein loading of hydroxyapatite." *Materials Technology* x; x(x), xx-xx. DOI: 10.1179/1753555715Y.0000000048

Final corrected proof is available at http://www.maneyonline.com

Present address: [1] Univ. Estadual Paulista, Faculty of Science, Laboratory of anelasticity and biomaterials, Bauru 17033-360, SP, Brazil; [2] Katholieke Universiteit Leuven, Department of Metallurgy and Materials Engineering, Heverlee 3001, Belgium; [2] Galephar S.A., Marche en Famenne 6900, Belgium.

1. Introduction

Oral delivery of therapeutic antigens (*e.g.* proteins, peptides) using nano or micron sized carriers is an alternative for parenteral administration methods which leads to enhanced patient convenience and compliance.[1,2] Carrier mediated antigen delivery has shown enhanced bioavailability as compared to soluble antigens.[3-5] The physico-chemical properties of the carrier material play a major role in determining the cellular uptake of the administered antigen. This makes some of the inorganic carriers like calcium phosphate or mesoporous silica appealing due to their biocompatibility and surface modification possibilities.[6-9] However inorganic carriers used as carriers are still in the pre-clinical stage and extensive research is necessary to assess their potential, as compared to the performance of polymeric carriers.[10] Enhanced protein loading on the inorganic carrier is one such property to be studied carefully which deals with the surface properties of the carrier material. Understanding the interaction mechanism and thus controlling the protein adsorption and release will also contribute to the bone implant materials development.[11]

The complex process of proteins adsorption onto solid surfaces is governed by forces like electrostatic, van der Waals and hydrophobic interactions.[12] Various advanced physical and chemical surface engineering methods are reported in order to increase the protein adsorption on inorganic materials, to make them conducive for various applications like protein delivery, protein purification, waste water treatment, etc.[13-17] A common platform for surface functionalisation with catechol containing molecules [e.g. 3,4-dihydroxy-L-phenylalanine (DOPA), dopamine (DA), norepinephrine (NA)] was reported on a variety of materials, including metal oxides, polymers and glass materials.[18,19] Oxidative polymerization of dopamine (DA) – a structural analogue of DOPA, was reported by Herlinger et al.[20] and has been exploited in several applications including under water adhesives, non-fouling coatings,

This is an author postprint version of the article published as: V. Ozhukil Kollath,,, S. Mullens, J. Luyten,, K. Traina, and R. Cloots. "Effect of DOPA and dopamine coupling on protein loading of hydroxyapatite." *Materials Technology* x; x(x), xx-xx. DOI: 10.1179/1753555715Y.0000000048

sensors, biomedical systems.[18,21,22] Nevertheless, reports of their use for inorganic carrier functionalisation are limited.[23,24] This study aims at increasing the protein loading on hydroxyapatite (HA) particles using DOPA and DA as linkers and improves the knowledge on the protein interaction.

Although oxidative polymerisation of these monomers has been reported, the exact mechanism is yet to be elucidated.[25-27] Despite the use of these molecules in several applications including under water adhesives, non-fouling coatings, sensors, biomedical systems,[18,21,22,28] their use as a linker for protein adsorption on inorganic materials (e.g. calcium phosphate) is still under-explored.[23,24] Researchers have tried to understand the protein adsorption on such materials by controlling the electrostatic and hydrophobic interactions.[29,30] This study aims at increasing the protein loading on hydroxyapatite (HA) particles, using DOPA and DA and elucidates the protein interactions involved.

The choice of carrier material was made because of HA's known biocompatibility.[9,31,32] Bovine serum albumin (BSA) was used as model protein in this study. HA powder samples were functionalized with DOPA and DA solutions at pH 8.5. The influence of the functionalisations on the BSA adsorption isotherms (at pH 7.1) was analysed. The adsorption isotherms were fitted to Langmuir and Freundlich adsorption models. Further characterization comprised zetapotential measurements, X-ray photon spectroscopy (XPS), Raman spectroscopy and thermogravimetric analysis on line coupled with mass spectrometry (TGA-MS).

2. Experimental methods

Hydroxyapatite (HA) powder was purchased from Merck (Prod. No.: 1.02196; Darmstadt, Germany). Bovine serum albumin (BSA), Bradford reagent, Tris(hydroxymethyl)aminomethane (TRIS), 3,4-Dihydroxy-L-phenylalanine (DOPA) and

Dopamine hydrochloride (DA) were purchased from Sigma-Aldrich. Highly pure water (Elix, Millipore) was used as solvent unless otherwise specified. All experiments were performed at room temperature.

For the DOPA and DA functionalisation, an aqueous solution of 2 mg ml^{-1} was prepared in 0.1 M TRIS-HCl buffer (pH=8.5). Two ml of these solutions were mixed with 0.2 g of HA. These suspensions were stirred magnetically for 2 h. After stirring, all the suspensions were centrifuged at 4000 rpm for 10 min (Centrifuge 5810, Eppendorf) in polypropylene centrifuge tubes. The supernatants were decanted and 2 ml of milliQ water was added to each tube to disperse the powder with the aid of a vortex mixer to wash off any loosely bound molecules. The tubes were centrifuged again at 4000 rpm for 10 minutes and supernatants were decanted. The residual paste in the tubes was dried at 40 °C during 48 h in a drying oven, before characterization.

Both the bare and functionalised HA powders were treated equally for the protein adsorption and pH was kept equal to 7.1 in all cases. The pH of suspensions was adjusted to 7.1 for functionalized powders by adding 0.01 M HCl. For BSA adsorption, a 2 hr adsorption time was selected from experience.[15] The adsorption experiments were performed by magnetically stirring a 10% w/v suspension of HA powder in BSA solutions (2 ml) of varying concentrations (from 0 to 20 mg ml^{-1}). Afterwards, the solution was centrifuged (Centrifuge 5810, Eppendorf AG, Germany) at 4000 rpm for 6 min (in swing bucket rotor) and then at 11 000 rpm for 15 min (in fixed angle rotor). The residual paste of the suspension was then dried in air during 24 h. Bradford assay was used to quantify the remaining BSA in the supernatant. The total amount of BSA adsorbed on the powder was obtained from the difference between initial and final (supernatant) concentrations of BSA in the solution. All adsorption measurements are represented as average values of at least duplicate experiments.

This is an author postprint version of the article published as: V. Ozhukil Kollath,,, S. Mullens, J. Luyten,, K. Traina, and R. Cloots. "Effect of DOPA and dopamine coupling on protein loading of hydroxyapatite." *Materials Technology* x; x(x), xx-xx. DOI: 10.1179/1753555715Y.0000000048

Thermogravimetric analyses (TGA) were performed (STA 449C, Netzsch) coupled to an online mass spectrometer (OmniStar GSD 301 O2, Pfeiffer Vacuum) in dry air atmosphere. Differential of the TG spectra provides the temperature of each weight loss events. Zeta potential measurements (Zetaprobe Analyzer, Colloidal Dynamics) were performed in the pH range 5-10 and the titrations were performed using HNO_3 (0.1 M) and NaOH (0.1 M). The Raman spectrum was acquired using Dilor XY in combination with and Olympus microscope (objective 50x). Green laser of 514 nm was used at 25 mW for 60 s during each acquisition. Elemental composition was analysed using X-ray photo electron spectroscopy (XPS) and atomic percentages were calculated using the software provided by the manufacturer (Thetaprobe, Thermo electron corporation).

3. Results and discussion

Figure 1 shows the influence of the DOPA and DA functionalisation on the BSA adsorption isotherms. The maximum adsorption of BSA on DA-HA increased 63 % as compared to the bare HA. On the contrary, the DOPA functionalisation did not significantly change the BSA isotherm. The zetapotential measurements as a function of the pH (Figure 2) showed the changes in surface charge and isoelectric point (IEP) of HA powder after functionalisation. No statistically relevant shift in zetapotential is measured after DA-functionalisation (IEP of 7.5 for DA-HA as compared to 7.3 for the bare HA powder). After DOPA functionalisation, the zetapotential curve is shifted towards more negative zetapotential values and the IEP is lowered to acidic pH (5.3).

Figure 1

Figure 2

It is known from literature that, in alkaline pH, DA will oxidize to quinone structure and subsequently polymerize to form polydopamine (PDA) (scheme S1a; supplementary material 1).[18] Apart from the brownish colour change of the powder, Raman spectroscopy indicated the presence of PDA with characteristic broad peaks at 1604 and 1412 cm^{-1} (figure S1; supplementary material 1).[33,34] Preferentially the catechol groups link with the hydroxyl and calcium ions on the HA surface. The final PDA structure contains no accessible functional groups which can dissociate and change the zetapotential. The shift in IEP of DOPA-HA to the acidic pH is indicative of the presence of carboxylic functional groups on the particle surface. Assuming the catechol groups are interacting with the HA surface, the total surface charge is originating from the carboxyl groups of the dihydroxy-indole monomers (scheme S1b; supplementary material 1). Within the pH range 3-8, the carboxyl group is deprotonated (table S1; supplementary material 1).[35] Hence the shift in zetapotential towards negative values (figure 2) indicates that the carboxylate group is electrostatically active on the surface of DOPA functionalized HA.

TGA-MS (figure 3) were used to quantitatively measure the amount of DA and DOPA adsorbed on the HA powder. After DA functionalisation, the TGA curve shows an additional weight loss in the temperature range from 200 to 520 °C, with DTG (differential thermogravimetry) maxima at 300 °C and 424 °C. On line MS detected the release of CO_2 (m/z = 44) and H_2O (m/z = 18) in the temperature range from 180 °C to 520 °C, assigned to the oxidation of the DA. A similar TGA profile was observed for DOPA-HA with DTG maxima at 314, 420 and 434 °C, assigned to the DOPA oxidation. The weight losses attributed to the oxidation are used to calculate the amount of DA and DOPA (table S2; supplementary material 1): 3.7 E-5 mol g^{-1} of powder was calculated for the DOPA

functionalisation compared to 3.2 E-5 mol g^{-1} of powder for the DA functionalisation. Additionally to the quantitative analysis by TGA-MS, XPS was performed to measure the surface elemental composition (table S3; supplementary material 1). For DA-HA, 0.6 at. % of nitrogen was measured. This result reinforces the idea that the functionalisation occurred.

Figure 3

The combined characterization from zetapotential measurements, Raman spectroscopy and thermogravimetry offers us clues to the adsorption mechanism of BSA onto the functionalized HA. As the zetapotential as function of the pH does not change after DA functionalisation, it can be concluded that the total Coulomb interaction between protein and surface remains unchanged as compared with bare HA. However, the presence of PDA on the surface offers the possibility for covalent linking by a Michael addition or Schiff base reaction mechanism with the amine groups of BSA.[18,36] Possible sites for Michael and Schiff base reactions are shown in scheme S1 (supplementary material 1). Also the decrease in hydrophilicity of the surface after PDA functionalisation could be contributing to the increase in BSA adsorption.[18,37] Despite the increase of the repulsive electrostatic interaction after DOPA functionalisation, the BSA adsorption isotherm is similar to that of bare HA. Apart from electrostatic interactions, DOPA molecules on the HA surface can interact with BSA via Michael addition as reported earlier.[38] Thus the adsorption mechanism between BSA and DOPA-HA powder is a combination of electrostatic and covalent interactions.

Indications of this stronger bonding of BSA with polymerized dopamine can also be found in the TGA profile. Figure 4 compares the weight loss as function of the temperature for BSA adsorbed on HA and on DA-HA. The thermal decomposition of BSA adsorbed on HA is a 2-

steps process, with DTG maxima at 323 °C and 450 °C.[39] The first weight loss is assigned to the oxidation and thermal decomposition of adsorbed BSA with the release of CO_2 (m/z=44), H_2O (m/z=18), NO and/or amines (m/z=30) and traces of aromatic compounds (m/z=77) (data not shown). The weight loss with DTG maximum at 450 °C can be attributed to the combustion of the char with formation of only CO_2 and NO (m/z=30). In case of DA-HA, the second DTG maximum is shifted to 470 °C. This shift of about 20 °C might indicate a stronger interaction of BSA after functionalisation.

The differences in adsorption mechanisms after DA and DOPA functionalisation also emerge from fitting the adsorption isotherms to the Langmuir and Freundlich models (table S4). The adsorption isotherms of bare HA and DOPA-HA are described more closely by the Langmuir model. After DA functionalisation, the Freundlich model is in better agreement with the experimental data. These data indicate the formation of BSA multilayer on DA-HA.

Figure 4

When normalizing the maximum BSA adsorption by the surface area (table S4) and comparing it with calculated values of full surface coverage, information is obtained on the conformation of the BSA on the surface. It has been reported that BSA can adsorb either in a *side-on* or *end-on* mode, with full surface coverage amounts of 172 and 309 ng cm^{-2} respectively in case of random adsorption.[40] This random adsorption model accounts 54.7 % of jamming limit and hence a loosely packed layer. In case of BSA adsorption on HA or DOPA-HA, the maximum adsorption amounts are below the calculated monolayer amounts for side-on adsorption. But in case of BSA adsorbed on DA-HA, the maximum BSA corresponds to the random side-on monolayer threshold.

4. Conclusions

In summary, the interaction of BSA with DOPA and DA functionalized HA was studied. Protein loading on DA-HA powder increased by 63 % as compared to the bare HA powder. The wide range of characterization tools and the comparison with theoretical models yielded more insight in the complex adsorption mechanisms involved. However, more research is needed to clarify all aspects of the polymerisation mechanism of DA and DOPA. Future work will focus on comparing the current method with other linker molecules to enhance the BSA adsorption as well as the protein release properties of the developed materials.

Acknowledgements

The authors gratefully acknowledge Ir. K Baert, Prof. I Vandendael (SURF, Vrije Universiteit Brussel) for Raman spectroscopy; Dr. B G De Geest, Prof. J P Remon (Laboratory of Pharmaceutical Technology, Ghent University) and Dr. V. Meynen (Laboratory of adsorption and catalysis, University of Antwerp) for fruitful discussions. VOK wish to thank VITO and University of Liège for financial assistance; and M. Sharma for proof reading the manuscript.

References

1. Grenha: *J. Pharm. Bioall. Sci.*, 2012, **4**, 95.
2. M. L. Hoffman-Terry, H. S. Fraimow, T. R. Fox, B. G. Swift and J. E. Wolf: *Am. J. Med.*, 1999, **106**, 44.
3. M. Singh and D. O'Hagan: *Nat. Biotechnol.*, 1999, **17**, 1075-1081.
4. S. De Koker, B. N. Lambrecht, M. A. Willart, Y. Van Kooyk, J. Grooten, C. Vervaet, J. P. Remon and B. G. De Geest: *Chem. Soc. Rev.*, 2011, **40**, 320-339; M. Dierendonck, S. De Koker, C. Cuvelier, J. Grooten, C. Vervaet, J. P. Remon and B. G. De Geest: *Angew. Chem., Int. Ed.*, 2010, **49**, 8620-8624.
5. L. J. De Cock, S. De Koker, B. G. De Geest, J. Grooten, C. Vervaet, J. P. Remon, G. B. Sukhorukov and M. N. Antipina: *Angew. Chem., Int. Ed.*, 2010, **49**, 6954-6973.
6. E. V. Giger, J. Puigmartí-Luis, R. Schlatter, B. Castagner, P. S. Dittrich and J. –C. Leroux: *J. Contr. Release*, 2011, **150**, 87-93.
7. M. Vallet-Regí, F. Balas and D. Arcos: *Angew. Chem., Int. Ed.*, 2007, **46**, 7548-7558.
8. G. Bhakta, S. Mitra and A. Maitra: *Biomaterials*, 2005, **26**, 2157-2163.
9. V. V. Sokolova, I. Radtke, R. Heumann and M. Epple: *Biomaterials*, 2006, **27**, 3147-3153.
10. Z. P. Xu, Q. H. Zeng, G. Q. Lu and A. B. Yu: *Chem. Eng. Sci.*, 2006, **61**, 1027-1040.

11. S. Tarafder, S. Banerjee, A. Bandyopadhyay and S. Bose: *Langmuir*, 2010, **26**, 16625-16629.
12. M. Rabe, D. Verdes and S. Seeger: *Adv. Colloid Interface Sci.*, 2011, **162**, 87-106.
13. K. Cai, M. Frant, J. Bossert, G. Hildebrand, K. Liefeith and K. D. Jandt: *Colloids Surf. B*, 2006, **50**, 1-8.
14. D. Kozlova, S. Chernousova, T. Knuschke, J. Buer, A. M. Westendorf and M. Epple: *J. Mater. Chem.*, 2011, **22**, 396-404.
15. V. Ozhukil Kollath, B. G. De Geest, S. Mullens, S. De Koker, J. Luyten, R. Persoons, K. Traina,. J. P. Remon and R. Cloots: *Adv. Eng. Mater.*, 2013, **15**, 295-301.
16. V. Ozhukil Kollath, S. Put, S. Mullens, A. Vanhulsel, J. Luyten, K. Traina and R. Cloots: *Plasma Process Polym*, 2015, DOI: 10.1002/ppap.201400092.
17. V. Ozhukil Kollath, F. Van den Broeck, K. Fehér, J. C. Martins, J. Luyten, K. Traina, S. Mullens and R. Cloots: *Chem: A Eur J*, 2015, DOI: 10.1002/chem.201500223.
18. H. Lee, S. M. Dellatore, W. M. Miller and P. B. Messersmith: *Science*, 2007, **318**, 426-430; B. P. Lee, P. B. Messersmith, J. N. Israelachvili and J. H. Waite: *Annu. Rev. Mater. Res.*, 2011, **41**, 99-132.
19. S. M. Kang, J. Rho, I. S. Choi, P. B. Messersmith and H. Lee: *J. Am. Chem. Soc.*, 2009, **131**, 13224-13225.
20. E. Herlinger, R. F. Jameson and W. Linert: *J. Chem. Soc., Perkin Trans.*, 1995, **2**, 259-263.
21. Q. Ye, F. Zhou and W. Liu: *Chem. Soc. Rev.*, 2011, **40**, 4244–4258.
22. J. Sedó, J. Saiz-Poseu, F. Busqué and D. Ruiz-Molina: *Adv. Mater.*, 2013, **25**, 653-701.
23. Y. Lee, S. H. Lee, J. S. Kim, A. Maruyama, X. Chen and T. G. Park: *J Control. Release*, 2011, **155**, 3-10.
24. G. Marcelo, A. Muñoz-Bonilla, J. Rodríguez-Hernández and M. Fernández-García: *Polym. Chem.*, 2013, **4**, 558-567.
25. M. d'Ischia, A. Napolitano, A. Pezzella, P. Meredith and T. Sarna: *Angew. Chem. Int. Ed.*, 2009, **48**, 3914-3921.
26. D. R. Dreyer, D. J. Miller, B. D. Freeman, D. R. Paul and C. W. Bielawski: *Langmuir*, 2012, **28**, 6428-6435.
27. S. Hong, Y. S. Na, S. Choi, I. T. Song, W. Y. Kim and H. Lee: Adv. Functional Mater., 2012, **22**, 4711-4717.
28. J. I. Lim, J. H. Kim and H. –K. Park: *Mater. Lett.*, 2012, **81**, 251-253.
29. F. Meder, T. Daberkow, L. Treccani, M. Wilhelm, M. Schowalter, A. Rosenauer, L. Mädler and K. Rezwan: *Acta Biomater.*, 2012, **8**, 1221-1229.
30. S. Dasgupta, A. Bandyopadhyay and S. Bose: *Acta Biomater.*, 2009, **5**, 3112-3121.
31. H. Fu, M. N. Rahaman, D. E. Day and R. F. Brown: *J. Mater. Sci.: Mater. Med.*, 2011, **22**, 579-591.
32. R. Ramachandran, W. Paul and C. P. Sharma: *J. Biomed. Mater. Res.*, 2009, **88B**, 41-48.
33. N. G. Rim, S. J. Kim, Y. M. Shin, I. Jun, D. W. Lim, J. H. Park and H. Shin: *Colloids Surf.*, 2012, B **91**, 189-197.
34. J. Ryu, S. H. Ku, H. Lee and C. B. Park: *Adv. Funct. Mater.*, 2010, **20**, 2132-2139.
35. X. Chen, J. Xie, C. Li, Z. Hu and X. Chen: *J. Sep. Sci.*, 2007, **27**, 1005-1010.
36. Cheng, S. Nie, S. Li, H. Peng, H. Yang, L. Ma, S. Sun and C. Zhao: *J. Mater. Chem. B*, 2013, **1**, 265-275.
37. J. –Y. Yoon, J. –H. Kim and W. –S. Kim: *Colloids Surf., B*, 1998, **12**, 15-22.
38. M. Yu, J. Hwang and T. H. Deming: *J. Am. Chem. Soc.*, 1999, **121**, 5825-5826.
39. T. –Y. Liu, S. –Y. Chen, D. –M. Liu and S. –C. Liou: *J. Contr. Release*, 2005, **107**, 112-121.

40. Mueller, M. Zacharias and K. Rezwan: *Adv. Eng. Mater.*, 2010, **12**, B53-61.

Captions:

Figure 1: BSA adsorption isotherms of bare and functionalized HA (Colour figure available online).

Figure 2: Zetapotential titration curves of HA, DOPA-HA and DA-HA (Colour figure available online).

Figure 3: TG/DTG and mass spectra of bare and functionalized HA powders. Curves with closed symbols represent TG and open symbols represent DTG spectra respectively. The mass spectra represent H_2O (m/z = 18) and CO_2 (m/z = 44) release during the process (Colour figure available online).

Figure 4: TG and DTG spectra of BSA on bare and DA functionalized HA. Curves with closed symbols represent TG and open symbols represent DTG spectra respectively (Colour figure available online).

Figure 1

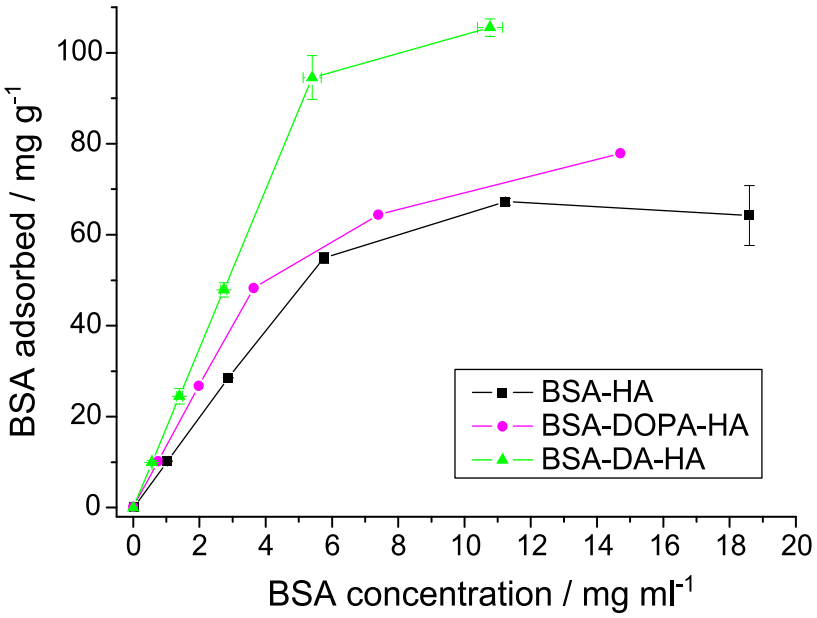

This is an author postprint version of the article published as: V. Ozhukil Kollath,,, S. Mullens, J. Luyten,, K. Traina, and R. Cloots. "Effect of DOPA and dopamine coupling on protein loading of hydroxyapatite." *Materials Technology* x; x(x), xx-xx. DOI: 10.1179/1753555715Y.0000000048

Figure 2

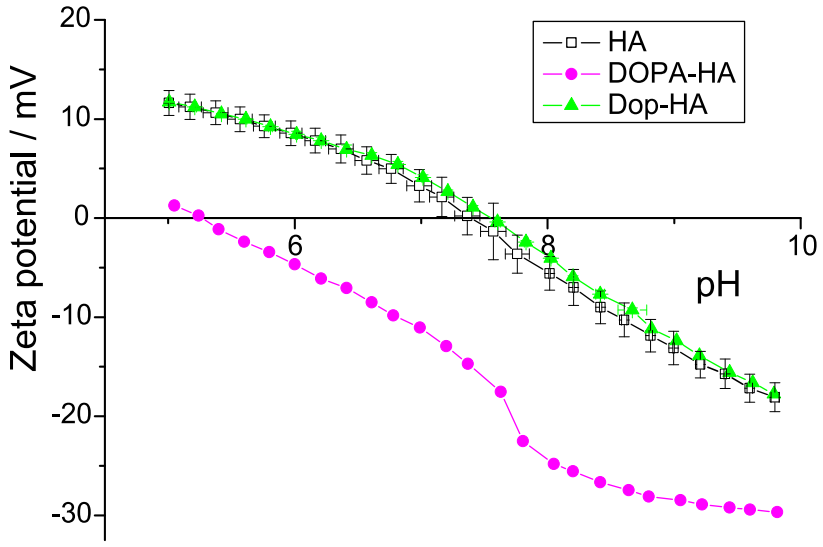

This is an author postprint version of the article published as: V. Ozhukil Kollath,,, S. Mullens, J. Luyten,, K. Traina, and R. Cloots. "Effect of DOPA and dopamine coupling on protein loading of hydroxyapatite." *Materials Technology* x; x(x), xx-xx. DOI: 10.1179/1753555715Y.0000000048

Figure 3

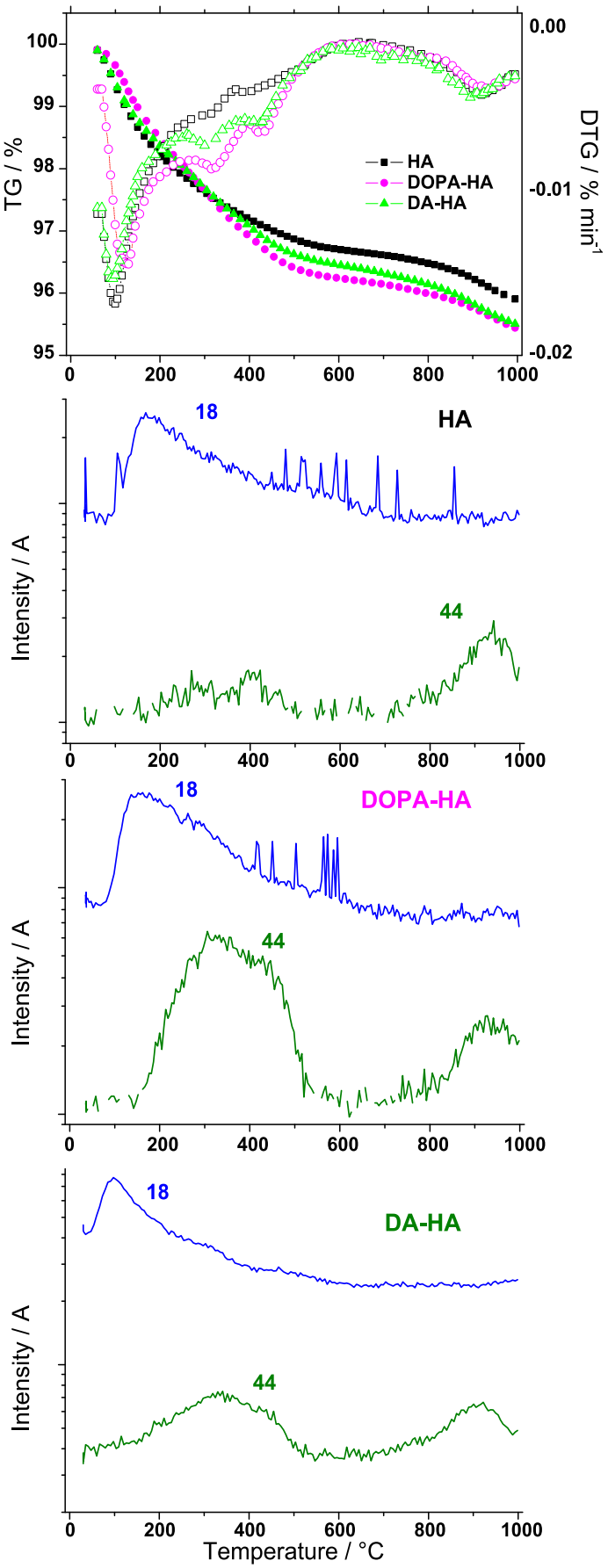

Mullens, J. Luyten,, K. Traina, and R. Cloots. "Effect of DOPA and dopamine coupling on protein loading of hydroxyapatite." *Materials Technology* x; x(x), xx-xx. DOI: 10.1179/1753555715Y.0000000048

This is an author postprint version of the article published as: V. Ozhukil Kollath,,, S. Mullens, J. Luyten,, K. Traina, and R. Cloots. "Effect of DOPA and dopamine coupling on protein loading of hydroxyapatite." *Materials Technology* x; x(x), xx-xx. DOI: 10.1179/1753555715Y.0000000048

Figure 4

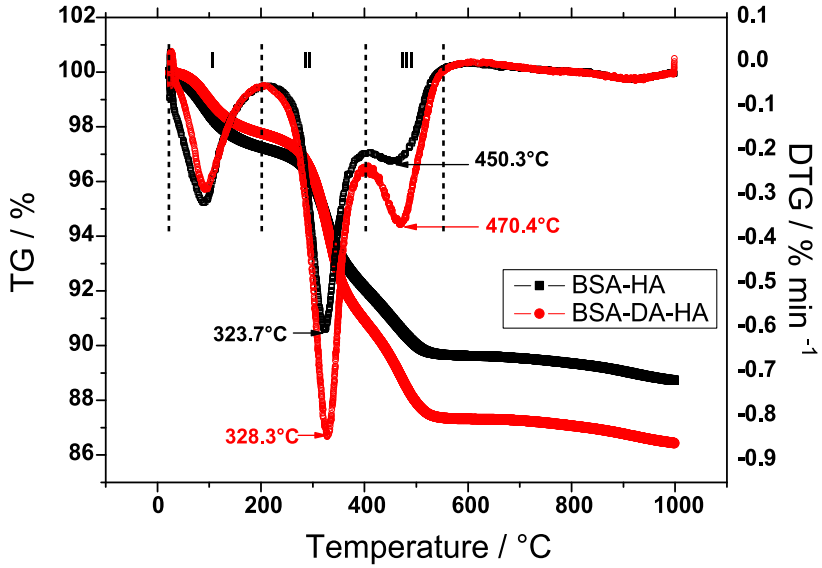

This is an author postprint version of the article published as: V. Ozhukil Kollath,,, S. Mullens, J. Luyten,, K. Traina, and R. Cloots. "Effect of DOPA and dopamine coupling on protein loading of hydroxyapatite." *Materials Technology* x; x(x), xx-xx. DOI: 10.1179/1753555715Y.0000000048

Supplementary Material 1

Effect of DOPA and dopamine coupling on the protein loading of hydroxyapatite

Vinayaraj Ozhukil Kollath,* Steven Mullens, Jan Luyten, Karl Traina and Rudi Cloots*

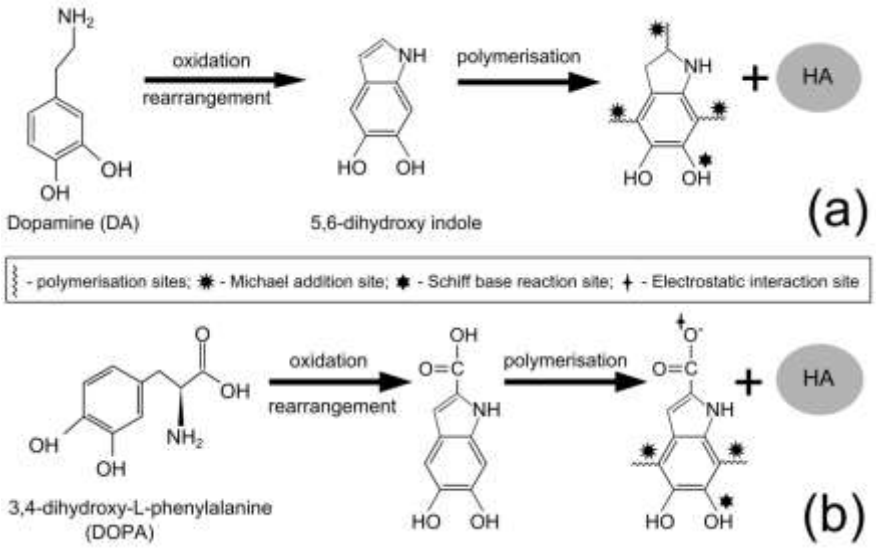

Scheme S1 Suggested functionalisation mechanisms on (a) DA-HA and (b) DOPA-HA

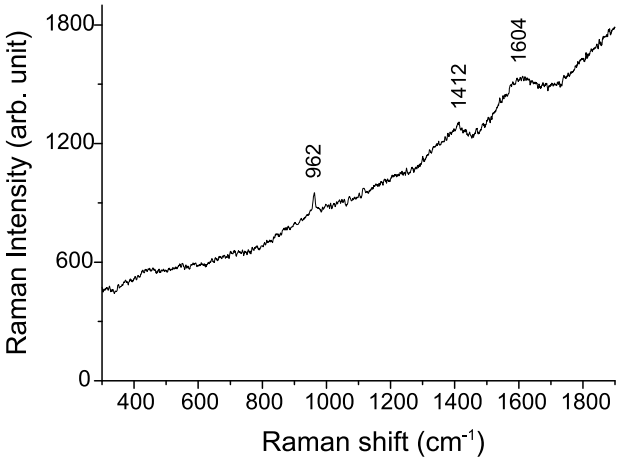

Fig. S1. Raman spectrum of DA-HA dry powder. The characteristic peaks of HA (962 cm^{-1}) and polydopamine (1604, 1412 cm^{-1}) were less intense due to the fluorescence from the sample.

Table S1. Dissociation constants of the ionisable groups of DOPA and DA.[1-3]

	pKa_1 (α-C-COOH)	pKa_2 (α-C-NH_3^+)	pKa_3-pKa_4 (OH_1-OH_2)	IEP
DOPA	2.3	8.1	9.9-11.8	5.2
DA	/	8.8	10.4-13.1	9.6

IEP – Isoelectric point.

This is an author postprint version of the article published as: V. Ozhukil Kollath,,, S. Mullens, J. Luyten,, K. Traina, and R. Cloots. "Effect of DOPA and dopamine coupling on protein loading of hydroxyapatite." *Materials Technology* x; x(x), xx-xx. DOI: 10.1179/1753555715Y.0000000048

Table S2. Percentage weight loss and the corresponding amount of DOPA and DA calculated from TGA

Sample	Mass loss during 220-520 °C (%)	Amount adsorbed HA (mol g^{-1})
DOPA-HA	0.73	3.70 E-5
DA-HA	0.48	3.22 E-5

Table S3. Elemental analysis of DA-HA using X-ray photoelectron spectroscopy (XPS)

Element	C1s	N1s	O1s	Ca2p	P2p
At. %	15.9	0.6	48.5	20.1	15.0

Table S4. Calculated values of theoretical adsorption models and maximum BSA adsorption values at 10 mg ml^{-1} BSA concentration to compare the random *side-on* adsorption value[‡] reported by Mueller et al.[6]

	Langmuir			Freundlich			BSA adsorbed
	Q_max	K_L	R^2	n	K_F	R^2	ng cm^{-2}
BSA/HA	90,99	0,167	0,9223	1,508	12,489	0,8952	106
BSA/DOPA-HA	105,71	0,197	0,9494	1,450	15,206	0,9361	111
BSA/DA-HA	228,83	0,091	0,8021	1,184	18,113	0,9635	167

[‡]Maximum BSA adsorption value calculated by random *side-on* adsorption model[4] = 172 ng cm^{-2}

SI References

1. X. Chen, J. Xie, C. Li, Z. Hu and X. Chen, *J Sep Sci*, 2004, **27**, 1005.
2. L. Rover Júnior, J. C. B. Fernandes, G. de Oliveira Neto and L. T. Kubota, *J Electroanal Chem*, 2000, **481**, 34.
3. E. Herlinger, R. F. Jameson and W. Linert, *J Chem Soc, Perkin Trans 2*, 1995, 259.
4. B. Mueller, M. Zacharias and K. Rezwan, *Adv Eng Mater*, 2010, **12**, B53.